SCIENTIFIC REPORTS

OPEN

SUBJECT AREAS:
COMPUTER SCIENCE
APPLIED MATHEMATICS
CHEMICAL PHYSICS

Received
4 September 2014

Accepted
2 December 2014

Published
19 December 2014

Correspondence and requests for materials should be addressed to Z.Z.Z. (zhangzz@fudan.edu.cn)

Dynamics of semiflexible recursive small-world polymer networks

Yi Qi[1,2], Maxim Dolgushev[3] & Zhongzhi Zhang[1,2]

[1]School of Computer Science, Fudan University, Shanghai 200433, China, [2]Shanghai Key Laboratory of Intelligent Information Processing, Fudan University, Shanghai 200433, China, [3]Theoretical Polymer Physics, University of Freiburg, Hermann-Herder-Str.3, D-79104 Freiburg, Germany.

One of the fundamental issues in polymer physics is to reveal the relation between the structures of macromolecules and their various properties. In this report, we study the dynamical properties of a family of deterministically growing semiflexible treelike polymer networks, which are built in an iterative method. From the analysis of the corresponding dynamical matrix we derive the solution for its eigenvalues and their multiplicities, making use of a combined numerical and analytical approach. The eigenvalue spectra allow us to investigate the mechanical relaxation forms in depth for different values of the stiffness parameter. We observe that the dynamics of semiflexible networks is sensitive to the stiffness parameter. Our work paves a way to explore the structures of the highly symmetric polymers and provides a comprehensive understanding of the role of semiflexibility for the regular treelike networks which possess a small-world feature.

As a rapid developing discipline, polymer science has attracted much attention in the past few years, since it provides a powerful tool to study the macromolecules with various structures[1,2]. Currently, an important issue within the field of polymer science is to unveil how the underlying architecture of macromolecules affects their dynamic behaviors. Among various models, the Generalized Gaussian Scheme (GGS)[3], which extends the well-known Rouse model[4], has provided useful insights into many static and dynamic properties of the polymers. In particular, it has been successfully applied to a large variety of flexible polymer structures, such as dendrimers[5], mesh-like polymers[6,7], fractals[8–10], dendritic[11,12], regular hyperbranched structures[13,14], scale-free[15,16] and small-world[17,18] networks, and so on. All these examples are important representatives of different classes of hyperbranched macromolecules, which possess macroscopically distinguishable behavior. Experimentally, topological features of the materials are evident, despite the averaging, smoothing out character inherent due to the structural disorder or polydispersity in the relaxation measurements[19]. While the GGS approach provides a basic means for the relation of the structure to the physical properties of polymers, it neglects some realistic features such as excluded volume and polymer stiffness, which are very important especially for biological macromolecules (proteins, DNA, etc.)[20–22].

While for analytic theories the inclusion of the excluded volume remains to be a hard task, recently, there have been a considerable number of theoretical investigations on the dynamic properties of semiflexible polymers[23–29]. Extending pioneering works for linear chains[30,31] and stars[32], it was put forward as a framework for the arbitrary semiflexible treelike polymers (STP)[24], for the complex semiflexible loop polymers[25], and so on. In the theoretical approaches the semiflexiblility was introduced by restricting the orientations of the bonds, which can be monitored through the related stiffness parameters[23–32]. Under such additional restrictions, it turns out that these approaches provide a more realistic description of semiflexible polymers[23,29]. However, the price one has to pay for it is an increase of the complexity for an analytical solution of the problem. Indeed, the dynamical matrix of the semiflexible polymers, which couples the set of equations of motion, contains more non-vanishing elements than that of the fully-flexible polymers. Nevertheless, also in this case, based on the numerical and analytical methods, one can determine the spectra of the dynamical matrix, which allows one to study the dynamic properties of semiflexible polymers[33,34].

The main purpose of this article is to uncover the dynamic properties of the regular treelike polymer networks in the framework of the STP model[24]. For this, we investigate in the STP framework the mechanical relaxation properties for a family of recursive treelike polymer networks which display a small-world behavior[35]. We first analyze the structure of the corresponding dynamical matrix and derive and analyze its spectra. Based on them we investigate for large polymer structures the mechanical loss moduli $[G''(\omega)]$, which allows one to observe the dynamical behavior of polymeric systems at different scales[3,36,37]. By comparing the $[G''(\omega)]$ of the flexible

polymer networks with that of the corresponding semiflexible ones, we observe that the stiffness parameter has dramatic influence on the dynamic properties of the polymers, especially in the high-frequency domain. Here, the STP framework allows us to carry on an in-depth analysis of the interplay between the structure and the dynamics of the polymer system. In particular, following the scheme of Refs. 33, 34, we show that the eigenmodes of the fully-flexible recursive tree-like polymers keep their structures also in case when one introduces semiflexibility. This allows us to obtain analytic expressions for at least half of the corresponding eigenvalue spectra as a function of the stiffness parameter. It turns out that introducing semiflexibility leads to a reduction of the degeneracy of the spectra.

The report is structured as follows: Section Results introduces the construction of the recursive networks, whose dynamics is studied in the STP-framework. Here we also analyze the corresponding dynamical matrices, their eigenvectors and eigenvalue spectra, which allow us to calculate and to discuss the mechanical relaxation loss moduli $G''(\omega)$ for the polymer networks. Section Discussion summarizes our main results and conclusions. Finally, section Methods recalls briefly the tools which use in the report, namely, the STP-model[24] and the eigenmodes of the fully-flexible recursive treelike polymers[35].

Results

Network construction. We start by introducing a model for a class of treelike networks with exponential growth[35], which are constructed in a deterministic iterative way. We denote by U_g ($g \geq 0$) the deterministic treelike networks after g iterations. Then the networks can be generated as follows. Initially ($g = 0$), U_0 consists of an isolated node, called the central node. For $g = 1$, f (f is a natural integer) new nodes are generated connecting the central node to form U_1. For $g \geq 1$, U_g is obtained from U_{g-1} by adding f new nodes to each existing node in U_{g-1}. Fig. 1 illustrates schematically the construction process of a network for the particular case of $f = 3$ for the first several iterations.

According to the construction algorithm of U_g, it is easy to see that at each iteration g_i ($g_i \geq 1$) the number of newly generated nodes is $L(g_i) = f(f+1)^{g_i-1}$. Thus, the network order (i.e., the total number of nodes), N_g, at iteration g leads to

$$N_g = \sum_{g_i=0}^{g} L(g_i) = (f+1)^g. \tag{1}$$

The corresponding number of edges (bonds) at iteration g is $N_g - 1$, which holds for all treelike networks[38].

This class of networks displays typical features of macromolecules in the polymer science[5–18]. Their cumulative degree distribution $P_{\mathrm{cum}}(k)$, defined as the probability that the degree of a uniformly chosen node is greater than or equal to k, decays exponentially with k as $P_{\mathrm{cum}}(k) = (f+1)^{-\frac{k-1}{f}}$[35]. The average path length (APL), which represents the mean of the shortest distance between two nodes over all node pairs, increases logarithmically with the network size[35]. The diameter, defined as the maximum length of the shortest path between two nodes over all node pairs, also grows logarithmically with the network order[35]. The features of the APL and of the diameter indicate that this class of polymer networks shows small-world behavior[39]. In addition, the degree correlations of the networks depend on the functionality f. The network is uncorrelated for $f = 3$. And the network is assortative and disassortative when the functionality f is in the interval [1,2] and [4, ∞), respectively[35].

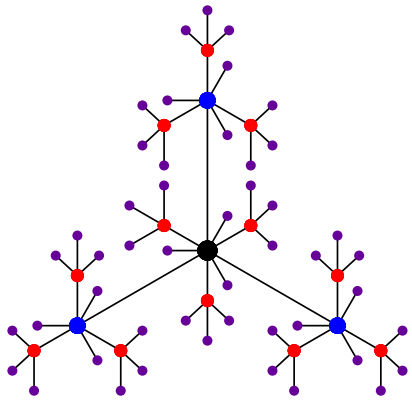

Figure 1 | Construction of the network U_g corresponding to $f = 3$ and $g = 3$.

After introducing the topological characteristics of the polymer networks, next we will investigate the dynamical properties on them, which is the primary topic of the present report.

Dynamics of semiflexible U_g. We start with a summary of the main formulas concerning the dynamics of semiflexible U_g; the details of the STP-model used here are provided in section Methods.

In the STP-framework[24], the semiflexibility is modeled through the complementary interactions between the next-nearest neighboring beads. In particular, one introduces the so-called stiffness parameters, which are related to the pairs of adjacent bonds. Exemplarily, the stiffness parameter q_i of bead i which connects bonds $\boldsymbol{l}_a$ and $\boldsymbol{l}_b$ is defined as $q_i \equiv \pm \langle \boldsymbol{l}_a \cdot \boldsymbol{l}_b \rangle / l^2$, where $\langle \ldots \rangle$ denotes an average, l^2 is the mean-square length of each bond, and the sign depends on the orientation of bonds. We note also that the beads of functionality $f_i = 1$ do not connect any pair of bonds, so that no stiffness parameters are associated with them, see section Methods for details.

The dynamics of the polymer networks is described by a set of Langevin equations[3,37], i.e., say, for the x-component of the position vector $\boldsymbol{r}_i = \{x, y, z\}$ one has:

$$\tau_0 \frac{\partial}{\partial t} x_i(t) + \sum_{j=1}^{N} A_{ij}^{\mathrm{STP}} x_j(t) = \tilde{f}_i(t) \Big/ K, \quad \forall i. \tag{2}$$

Here $\tau_0 = \zeta/K$, ζ is the friction constant, K is the spring constant (see also equation (45) in Methods). Moreover, $\tilde{f}_i(t)$ is the x-component of the usual fluctuating Gaussian force acting on the ith bead, for which $\left\langle \tilde{f}_i(t) \right\rangle = 0$ and $\left\langle \tilde{f}_i(t) \tilde{f}_j(t') \right\rangle = 2k_B T \zeta \delta_{ij} \delta(t-t')$ hold.

The interaction between the beads are described through the dynamical matrix $\mathbf{A}^{\mathrm{STP}} = \left(A_{ij}^{\mathrm{STP}}\right)$, whose entries are known in closed form[24]. Here it is worthwhile to introduce a notation to present the situation of the bead sites, see Fig. 2. Starting from an arbitrary bead i in the structure, we denote its neighbors by i_k and the neighbors of i_k by i_{ks}. The corresponding functionalities of beads i and i_k are f_i and f_{i_k} respectively, while the corresponding stiffness parameter of junctions i and i_k are q_i and q_k respectively. For these all the non-vanishing elements of the matrix $\mathbf{A}^{\mathrm{STP}}$ are given by:

$$A_{ii}^{\mathrm{STP}} = \frac{f_i}{1-(f_i-1)q_i} + \sum_{i_k} \frac{(f_{i_k}-1)q_{i_k}^2}{1-(f_{i_k}-2)q_{i_k}-(f_{i_k}-1)q_{i_k}^2}, \tag{3}$$

$$A_{ii_k}^{\mathrm{STP}} = -\frac{1-(f_i-1)(f_{i_k}-1)q_i q_{i_k}}{(1-(f_i-1)q_i)(1-(f_{i_k}-1)q_{i_k})}, \tag{4}$$

and

$$A_{ii_{ks}}^{\mathrm{STP}} = \frac{q_{i_k}}{1-(f_{i_k}-2)q_{i_k}-(f_{i_k}-1)q_{i_k}^2}. \tag{5}$$

whereas all other elements of $\mathbf{A}^{\mathrm{STP}}$ vanish[24].

Based on the structure of $\mathbf{A}^{\mathrm{STP}}$, equation (3) ~ (5), it is a simple matter to determine all elements of the matrix $\mathbf{A}_g^{\mathrm{STP}}$ for U_g. For simplicity, we assume that all beads of the same functionality f_i in the semiflexible polymer U_g have the same stiffness parameter q_i.

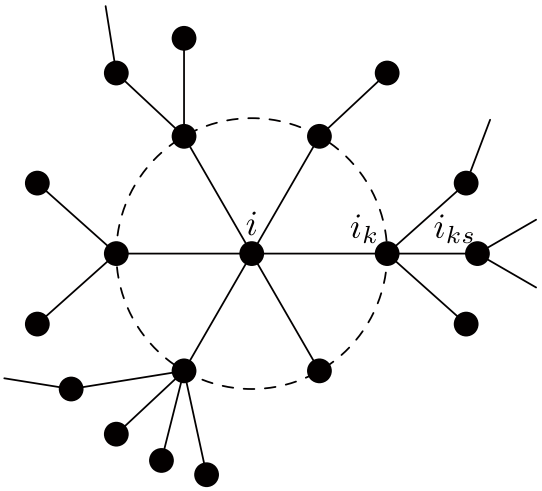

Figure 2 | Schematic drawing of the nearest and next-nearest neighbors of a bead *i* in a treelike network. Here we denote one of the nearest neighbors of bead i by i_k and one of the next nearest neighbors of bead i by i_{ks}.

Note that the peripheral beads of the polymer U_g have functionality $f_i = 1$ and hence do not connect any bonds, thus we only have to consider the stiffness parameter of inner beads. In the following, we assume that the stiffness parameter q_i of the inner bead i which has functionality $f_i (f_i > 1)$ is taken to be $q_i = \frac{q}{f_i - 1}$, where q is a real number between 0 and 1.

Now, we can categorize the diagonal elements into two different situations:

1. If i is a peripheral bead then $f_i^{(g)} = 1$. It is connected by a single neighbor i_k of functionality $f_{i_k}^{(g)}$ to the rest of the U_g. Thus, according to equation (3) the value of $\left(A_g^{\mathrm{STP}}\right)_{ii}$ follows:

$$\left(A_g^{\mathrm{STP}}\right)_{ii} = 1 + \frac{q^2}{\left(f_{i_k}^{(g)} - 1 + q\right)(1-q)}. \tag{6}$$

2. Otherwise, the bead i has functionality $f_i^{(g)} > 1$, hence the value of $\left(A_g^{\mathrm{STP}}\right)_{ii}$ turns out to be:

$$\left(A_g^{\mathrm{STP}}\right)_{ii} = \frac{f_i^{(g)}}{1-q} + \sum_{i_k \in \Delta_i^{(g)}} \frac{q^2}{\left(f_{i_k}^{(g)} - 1 + q\right)(1-q)}, \tag{7}$$

where the set $\Delta_i^{(g)}$ contains only the neighbor beads $\{i_k\}$ of bead i, which have functionality $f_{i_k}^{(g)} > 1$ in the gth generation.

As a second step we consider the non-diagonal nearest-neighboring (NN) elements of $\mathbf{A}_g^{\mathrm{STP}}$. There are also two distinct cases:

1. If either i or i_k is a peripheral bead. From equation (40) the value of $\left(A_g^{\mathrm{STP}}\right)_{ii_k}$ leads to:

$$\left(A_g^{\mathrm{STP}}\right)_{ii_k} = -\frac{1}{1-q}. \tag{8}$$

2. Otherwise, both two beads have functionality $f_i^{(g)} > 1$ and $f_{i_k}^{(g)} > 1$, so that $\left(A_g^{\mathrm{STP}}\right)_{ii_k}$ turns out to be:

$$\left(A_g^{\mathrm{STP}}\right)_{ii_k} = -\frac{1+q}{1-q}. \tag{9}$$

Finally, we have to determine the next nearest-neighboring (NNN) elements of $\left(A_g^{\mathrm{STP}}\right)_{ii_{ks}}$. These elements depend only on the bead i_k of

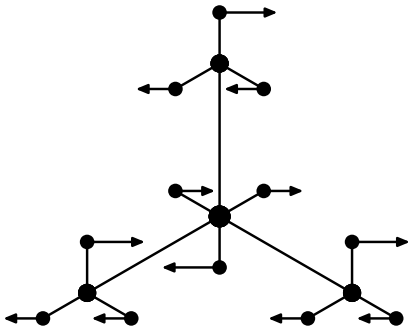

Figure 3 | Schematic drawing of the beads movement corresponding to the case when the inner beads are immobile. Here U_g has functionality $f = 3$ and generation $g = 2$. The sum of the amplitudes of all the f mobile beads generated by the same ascendant in the second generation vanishes.

functionality $f_{i_k}^{(g)}$ lying between the beads i and i_{ks}. From equation (41), the $\left(A_g^{\mathrm{STP}}\right)_{ii_{ks}}$ can take only one single value, which is

$$\left(A_g^{\mathrm{STP}}\right)_{ii_{ks}} = \frac{q}{\left(f_{i_k}^{(g)} - 1 + q\right)(1-q)}. \tag{10}$$

All other non-diagonal elements of the matrix $\mathbf{A}_g^{\mathrm{STP}}$ vanish.

According to the construction of U_g and the elements of $\mathbf{A}_g^{\mathrm{STP}}$ discussed above, it is easy to observe that the matrix $\mathbf{A}_g^{\mathrm{STP}}$ has the following block form:

$$\mathbf{A}_g^{\mathrm{STP}} = \begin{pmatrix} \mathbf{L}_g & \mathbf{B}_g & \mathbf{B}_g & \dots & \mathbf{B}_g \\ \mathbf{B}_g^{\mathrm{T}} & \mathbf{D}_g & \mathbf{C}_g & \dots & \mathbf{C}_g \\ \mathbf{B}_g^{\mathrm{T}} & \mathbf{C}_g & \mathbf{D}_g & \dots & \mathbf{C}_g \\ \vdots & \vdots & \vdots & \vdots & \vdots \\ \mathbf{B}_g^{\mathrm{T}} & \mathbf{C}_g & \mathbf{C}_g & \dots & \mathbf{D}_g \end{pmatrix}_{(f+1)\times(f+1)}, \tag{11}$$

where each block is a $(f+1)^{g-1} \times (f+1)^{g-1}$ matrix. Here $\mathbf{L}_g$ represents the $(f+1)^{g-1}$ inner beads. $\mathbf{C}_g$ and $\mathbf{D}_g$ correspond to the $f(f+1)^{g-1}$ peripheral beads. $\mathbf{B}_g$ describes the interaction between them.

Furthermore, to bead i, at each subsequent iteration, f new beads will be linked. Hence, the degree of bead i in the generation g evolves as:

$$f_i^{(g)} = f_i^{(g-1)} + f, \tag{12}$$

Thus, in the generation g, all the inner beads have functionalities larger than one. Therefore, from equation (7) all the diagonal ele-

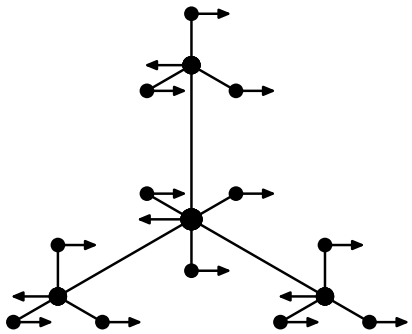

Figure 4 | Schematic drawing of the beads movement corresponding to the case when the inner beads are mobile. Here U_g has functionality $f = 3$ and generation $g = 2$. All the f mobile beads generated by the same ascendant in the second generation have same amplitude.

ments of matrix $\mathbf{L}_g$ are:

$$(L_g)_{ii} = \frac{f_i^{(g)}}{1-q} + \sum_{i_k \in \Delta_i^{(g)}} \frac{q^2}{\left(f_{i_k}^{(g)} - 1 + q\right)(1-q)}, \tag{13}$$

and the NN elements of matrix $\mathbf{L}_g$ are:

$$(L_g)_{ii_k} = -\frac{1+q}{1-q}. \tag{14}$$

Moreover, the NNN elements of $\mathbf{L}_g$ are determined as:

$$(L_g)_{ii_{ks}} = \frac{q}{\left(f_{i_k}^{(g)} - 1 + q\right)(1-q)}. \tag{15}$$

All other non-diagonal elements of the matrix $\mathbf{L}_g$ vanish.

Now, as can be inferred from the U_g construction, the structure of the matrix $\mathbf{B}_g$ takes the form:

$$\mathbf{B}_g = \begin{pmatrix} \mathbf{B}_g^{(1)} & \mathbf{B}_g^{(2)} & \mathbf{B}_g^{(2)} & \dots & \mathbf{B}_g^{(2)} \\ \mathbf{B}_g^{(3)} & \mathbf{B}_g^{(4)} & 0 & \dots & 0 \\ \mathbf{B}_g^{(3)} & 0 & \mathbf{B}_g^{(4)} & \dots & 0 \\ \vdots & \vdots & \vdots & \vdots & \vdots \\ \mathbf{B}_g^{(3)} & 0 & 0 & \dots & \mathbf{B}_g^{(4)} \end{pmatrix}_{(f+1)\times(f+1)}, \tag{16}$$

where each block is a $(f+1)^{g-2} \times (f+1)^{g-2}$ matrix. The component matrices $\mathbf{B}_g^{(2)}$, $\mathbf{B}_g^{(3)}$ and $\mathbf{B}_g^{(4)}$ are diagonal matrices. The matrix $\mathbf{B}_g^{(1)}$ obeys similar relations as matrix $\mathbf{B}_g$.

Furthermore, in equation (11) the block $\mathbf{C}_g$ represents the NNN interaction among the peripheral beads of the network. Therefore, its elements are given by equation (10). Moreover, $\mathbf{C}_g$ is a diagonal matrix. The main diagonal entries of $\mathbf{C}_g$ are given by

$$(C_g)_{11} = \frac{q}{(gf-1+q)(1-q)} \tag{17}$$

and by

$$(C_g)_{ii} = \frac{q}{((g-j+1)f+q)(1-q)}, \tag{18}$$

where $(1+f)^{j-2} < i \le (1+f)^{j-1}$ and $2 \le j \le g$.

Finally, let us consider the blocks $\mathbf{D}_g$, which are also diagonal matrices. According to equation (6) and the bead degree, the main diagonal entries of $\mathbf{D}_g$ can be expressed as:

$$(D_g)_{11} = 1 + \frac{q^2}{(gf-1+q)(1-q)} \tag{19}$$

and

$$(D_g)_{ii} = 1 + \frac{q^2}{((g-j+1)f+q)(1-q)}, \tag{20}$$

where $(1+f)^{j-2} < i \le (1+f)^{j-1}$ and $2 \le j \le g$.

Based on the structure of dynamical matrix $\mathbf{A}_g^{\mathrm{STP}}$ discussed above, in the next subsection, we will determine the eigenvalue spectra of this matrix.

Eigenvalue spectra of $\mathbf{A}_g^{\mathrm{STP}}$. In order to study the dynamical properties of the semiflexible polymer U_g, we will use the results of the previous subsections. In particular, the solution of the set of equations (2) requires diagonalization of $\mathbf{A}_g^{\mathrm{STP}}$. For several highly symmetric structures, such as dendrimers and Vicsek fractals, the set of eigenvalues can be obtained with the help of the similarity between the eigenvectors' structure of the fully flexible polymer and that of the corresponding semiflexible case[33,34], fact which also is of judicious use in case of U_g-networks. We develop our study of the eigenvalues of the semi-flexible polymers in three steps: First, in Methods we recall the spectra distribution of the fully flexible case; here we discuss the features of the corresponding eigenvectors and show that these features are also applicable to the semiflexible U_g polymers – we use a combined analytical and numerical approach to derive their eigenvalues.

Let $\boldsymbol{v}$ denote the eigenvector, whose corresponding eigenvalue is λ. $\boldsymbol{v}$ can be expressed as

$$\boldsymbol{v} = \begin{pmatrix} \boldsymbol{v}_1 \\ \boldsymbol{v}_2 \\ \boldsymbol{v}_3 \\ \vdots \\ \boldsymbol{v}_{f+1} \end{pmatrix}, \tag{21}$$

where all $\boldsymbol{v}_i$ of the vector $\boldsymbol{v}$ have same sizes. For fully-flexible U_g (see Methods), we distinguish between the following two cases:

In the first case, the vector $\boldsymbol{v}$ satisfies following relations:

$$\boldsymbol{v}_1 = 0, \tag{22}$$

$$\boldsymbol{v}_2 + \boldsymbol{v}_3 + \ldots + \boldsymbol{v}_{f+1} = 0. \tag{23}$$

Based on the above two expressions of the eigenvectors, one can readily observe that, in this case, only beads of highest generation can move, while their ascendants(inner beads) are immobile, see Fig. 3. Moreover, the sum of the amplitudes associated with the f mobile descendants, which are generated by arbitrary bead in the $(g-1)$th generation, vanishes.

In the second case, the vector $\boldsymbol{v}$ satisfies following relation:

$$\boldsymbol{v}_2 = \boldsymbol{v}_3 = \boldsymbol{v}_4 = \cdots = \boldsymbol{v}_{f+1}. \tag{24}$$

In this case, all of the f mobile descendants generated by the same bead in the $(g-1)$th generation have the same amplitude, see Fig. 4.

We make a brief summary by noticing that for U_g the eigenmotions of beads can be categorized into two groups: (i) Motions involving immobile inner beads. (ii) Motions involving mobile inner beads. As we proceed to show, this finding allows us to readily study the spectrum of the dynamical matrix in the corresponding semiflexible U_g polymers.

First we show that U_g have similar structure of eigenvectors in the fully-flexible and in semiflexible cases, i.e. we consider the following eigenvalue problem:

$$\mathbf{A}_g^{\mathrm{STP}} \boldsymbol{v} = \lambda \boldsymbol{v}, \tag{25}$$

where $\mathbf{A}_g^{\mathrm{STP}}$ is the dynamical matrix of U_g. Based on equation (11), equation (25) can be expressed as

$$\begin{pmatrix} \mathbf{L}_g & \mathbf{B}_g & \mathbf{B}_g & \dots & \mathbf{B}_g \\ \mathbf{B}_g^{\mathrm{T}} & \mathbf{D}_g & \mathbf{C}_g & \dots & \mathbf{C}_g \\ \mathbf{B}_g^{\mathrm{T}} & \mathbf{C}_g & \mathbf{D}_g & \dots & \mathbf{C}_g \\ \vdots & \vdots & \vdots & \vdots & \vdots \\ \mathbf{B}_g^{\mathrm{T}} & \mathbf{C}_g & \mathbf{C}_g & \dots & \mathbf{D}_g \end{pmatrix} \begin{pmatrix} \boldsymbol{v}_1 \\ \boldsymbol{v}_2 \\ \boldsymbol{v}_3 \\ \vdots \\ \boldsymbol{v}_{f+1} \end{pmatrix} = \lambda \begin{pmatrix} \boldsymbol{v}_1 \\ \boldsymbol{v}_2 \\ \boldsymbol{v}_3 \\ \vdots \\ \boldsymbol{v}_{f+1} \end{pmatrix}, \tag{26}$$

where vectors $\boldsymbol{v}_i (1 \le i \le f+1)$ are components of $\boldsymbol{v}$. Equation (26) leads to the following equations:

$$\begin{cases} \mathbf{L}_g\boldsymbol{v}_1+\mathbf{B}_g\boldsymbol{v}_2+\cdots+\mathbf{B}_g\boldsymbol{v}_{f+1}=\lambda\boldsymbol{v}_1 \\ \mathbf{B}_g^{\mathrm{T}}\boldsymbol{v}_1+\mathbf{D}_g\boldsymbol{v}_2+\cdots+\mathbf{C}_g\boldsymbol{v}_{f+1}=\lambda\boldsymbol{v}_2 \\ \qquad\qquad\qquad\vdots \\ \mathbf{B}_g^{\mathrm{T}}\boldsymbol{v}_1+\mathbf{C}_g\boldsymbol{v}_2+\cdots+\mathbf{D}_g\boldsymbol{v}_{f+1}=\lambda\boldsymbol{v}_{f+1} \end{cases}. \tag{27}$$

When the inner beads are immobile, the eigenvector $\boldsymbol{v}$ satisfies equations (22) and (23). Then the system (27) can be reduced to

$$\begin{cases} (\mathbf{D}_g-\mathbf{C}_g)\boldsymbol{v}_2=\lambda\boldsymbol{v}_2 \\ (\mathbf{D}_g-\mathbf{C}_g)\boldsymbol{v}_3=\lambda\boldsymbol{v}_3 \\ \qquad\vdots \\ (\mathbf{D}_g-\mathbf{C}_g)\boldsymbol{v}_f=\lambda\boldsymbol{v}_f \end{cases}. \tag{28}$$

Let $\mathbf{E}_g=\mathbf{D}_g-\mathbf{C}_g$ be the matrix that have the same size of $\mathbf{D}_g$ and $\mathbf{C}_g$, then $\mathbf{E}_g$ is also a diagonal matrix. The system (28) defines an eigenvalue problem which is corresponding to the following matrix:

$$\mathbf{AN}_g=\begin{pmatrix} \mathbf{E}_g & 0 & 0 & \cdots & 0 \\ 0 & \mathbf{E}_g & 0 & \cdots & 0 \\ 0 & 0 & \mathbf{E}_g & \cdots & 0 \\ \vdots & \vdots & \vdots & \vdots & \vdots \\ 0 & 0 & 0 & \cdots & \mathbf{E}_g \end{pmatrix}_{(f-1)\times(f-1)}. \tag{29}$$

Obviously, each eigenvalue of matrix $\mathbf{E}_g$ is also an eigenvalue of matrix $\mathbf{AN}_g$ with multiplicity $f-1$. As a real and diagonal matrix, $\mathbf{E}_g$ has exactly $(f+1)^{g-1}$ eigenvalues and the eigenvalues of matrix $\mathbf{E}_g$ is equivalent to the main diagonal entries of matrix $\mathbf{E}_g$.

Based on equations (17)-(20), the main diagonal entries of matrix $\mathbf{E}_g$ can be easily evaluated:

$$(E_g)_{11}=(D_g)_{11}-(C_g)_{11}=1-\frac{q}{gf-1+q} \tag{30}$$

and

$$(E_g)_{ii}=(D_g)_{ii}-(C_g)_{ii}=1-\frac{q}{(g-j+1)f+q}, \tag{31}$$

where $(1+f)^{j-2}<i\le(1+f)^{j-1}$ and $2\le j\le g$. From equation (30) and (31), there are g distinct eigenvalues of matrix $\mathbf{E}_g$, namely,

$$\lambda_1=1-\frac{q}{gf-1+q}, \tag{32}$$

whose multiplicity is 1 in the matrix $\mathbf{E}_g$ and $f-1$ in the matrix $\mathbf{A}_g^{\mathrm{STP}}$, and

$$\lambda_j=1-\frac{q}{(g-j+1)f+q}, \tag{33}$$

where $2\le j\le g$. The multiplicity of this eigenvalue is $(f+1)^{j-2}f$ in the matrix $\boldsymbol{E_g}$, while in the matrix $\mathbf{A}_g^{\mathrm{STP}}$ its multiplicity is

$$M_j=(f+1)^{j-2}f(f-1). \tag{34}$$

We now calculate the total number N_n of eigenvalues for the group that the inner beads are immobile

$$N_n=f-1+\sum_{i=2}^{g}(f-1)f(f+1)^{i-2}=(f-1)(f+1)^{g-1}. \tag{35}$$

A special case of equation (32) and (33) is the fully flexible case, for which q vanish. We observe that in this case $\lambda_1\to 1$ and $\lambda_j\to 1$, which corresponds to the eigenvalue set $FE1_g$ of the fully flexible case.

When the inner beads are mobile, the eigenvector $\boldsymbol{v}$ satisfies equation (24). Then equation (27) can be reduced to

$$\begin{cases} \mathbf{L}_g\boldsymbol{v}_1+f\mathbf{B}_g\boldsymbol{v}_2=\lambda\boldsymbol{v}_1 \\ \mathbf{B}_g^{\mathrm{T}}\boldsymbol{v}_1+(\mathbf{D}_g+(f-1)\mathbf{C}_g)\boldsymbol{v}_2=\lambda\boldsymbol{v}_2 \end{cases}, \tag{36}$$

which is equivalent to determining the eigenvalues of the following matrix:

$$\mathbf{AS}_g=\begin{pmatrix} \mathbf{L}_g & f\mathbf{B}_g \\ \mathbf{B}_g^{\mathrm{T}} & \mathbf{D}_g+(f-1)\mathbf{C}_g \end{pmatrix}, \tag{37}$$

in which each block is a $(f+1)^{g-1}\times(f+1)^{g-1}$ matrix and $\mathbf{AS}_g$ is a $2(f+1)^{g-1}\times 2(f+1)^{g-1}$ matrix. The diagonalization of matrices $\mathbf{AS}_g$ can be performed numerically. As discussed in previous subsection, $\mathbf{L}_g$ and $\mathbf{B}_g$ are sparse matrices, while $\mathbf{D}_g$ and $\mathbf{C}_g$ are diagonal matrices, that is to say, the matrix $\mathbf{AS}_g$ is considerably sparse, which is of great help to the diagonalization procedure.

In summary, the total number of eigenvalues corresponding to the group that inner beads are mobile is:

$$N_s=2(f+1)^{g-1}. \tag{38}$$

By summing those from group (i), equation (35), and, from group (ii), equation (38), we have

$$N_n+N_s=(f-1)(f+1)^{g-1}+2(f+1)^{g-1}=(f+1)^g\equiv N_g. \tag{39}$$

which indicates that we have found the all eigenvalues of U_g.

In order to demonstrate the influence of stiffness, we plot in Fig. 5 and Fig. 6 the distribution of the eigenvalue spectra for U_g. The left part and the right part of Fig. 5 display the eigenvalues in ascending order for U_g of $f=3$ and of $f=4$, respectively. From Fig. 5, it is easy to notice that with the increase of the stiffness parameter q, the large eigenvalues of the dynamical matrix grow, while the small ones decrease. By comparing the left part and the right part of Fig. 6, we observe that the number of distinct eigenvalues in the semiflexible U_g is higher than for its flexible counterparts. In case of U_g, the reason for this phenomenon lies in the the dynamical matrix, which has more non-vanishing elements for semiflexible U_g. However, one should note, that semiflexibilty not always leads to a different structure of the eigenvalue spectra. For example, the multiplicities of the eigenvalues for fully-flexible and for semiflexible dendrimers are the same[33].

Another feature which becomes apparent in both parts of Fig. 5 is that the eigenvalue $\lambda_g=\frac{f}{f+q}$, which is located in the in-between part of the spectra, has the highest multiplicity. As the stiffness parameter q decreases from 1 to 0, λ_g increases gradually and approaches 1 (Note that in the corresponding fully flexible network, this eigenvalue equals to 1 for any functionality). From equation (34) we know that the multiplicity of λ_g is $(f+1)^{(g-2)}f(f-1)$, which is increasing with functionality f and generation g. For U_g of any g, λ_g occupies exactly $[f(f-1)/(f+1)^2]$ part of the whole spectrum. For example, λ_g takes 3/8 part for $f=3$ and 12/25 part for $f=4$, respectively. As we will show, these differences of spectra between the two types of polymer networks U_g will lead to different dynamic behaviors.

To conclude this part, it turns out that the determination of eigenvalues discussed here is based on a judicious use of the typical bead motions in the highly symmetric polymers. This approach can provide analytical expressions of a large part of the spectra and their multiplicities in the semiflexible polymer network with arbitrary functionality and genaration. Instead of the traditional brute-force numerical diagonalization of the complete dynamical matrix, this approach considerably reduces the computational complexity of the eigenvalue problem and may pave the way for exploring other semiflexible polymers with complex topology, especially for symmetric architectures.

Mechanical relaxation. The eigenvalue spectrum $\{\lambda_k\}$ of $\mathbf{A}_g^{\mathrm{STP}}$ plays a fundamental role in the static and dynamic properties of

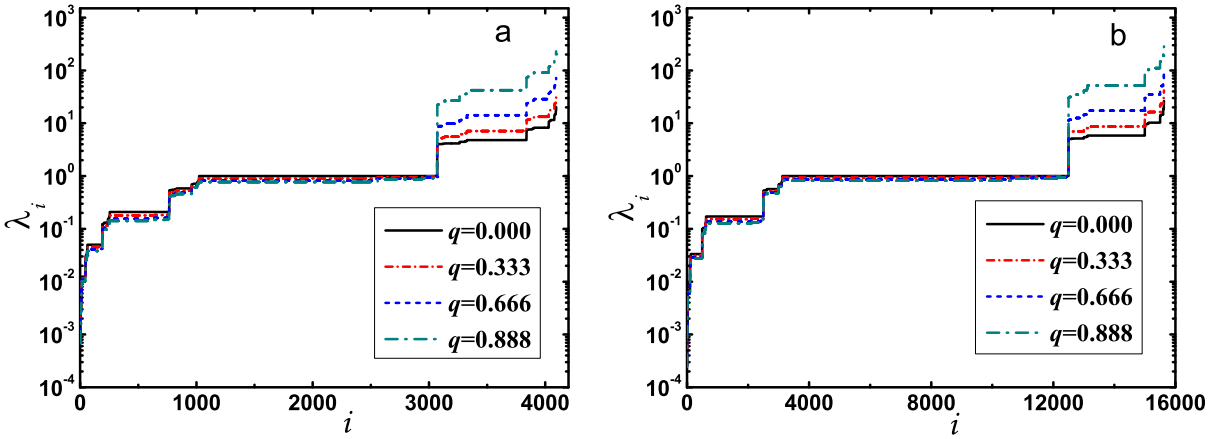

Figure 5 | Spectrum curves of polymer network U_g of generation $g = 6$ and functionality $f = 3$ (a) or $f = 4$ (b) for different degrees of stiffness q.

polymers[3,23]. In this report we focus on the mechanical relaxation, which is represented by the complex shear modulus[37]

$$G^*(\omega) = G'(\omega) + iG''(\omega), \tag{40}$$

where its real part $G'(\omega)$ and imaginary part $G''(\omega)$ are the storage modulus and the loss modulus respectively. The dimensionless storage $[G'(\omega)]$ and loss $[G''(\omega)]$ moduli are given by[3]

$$[G'(\omega)] = \frac{G'(\omega)}{\nu k_B T} = \frac{1}{N}\sum_{k=2}^{N} \frac{(\omega\tau_0/2\lambda_k)^2}{1+(\omega\tau_0/2\lambda_k)^2}, \tag{41}$$

and

$$[G''(\omega)] = \frac{G''(\omega)}{\nu k_B T} = \frac{1}{N}\sum_{k=2}^{N} \frac{\omega\tau_0/2\lambda_k}{1+(\omega\tau_0/2\lambda_k)^2}, \tag{42}$$

where τ_0 is as in in equation (2) and the $\{\lambda_k\}$ are the nonvanishing eigenvalues of the matrix $\mathbf{A}_g^{\mathrm{STP}}$.

Based on the eigenvalues discussed in the previous subsection, we calculate the reduced loss moduli $[G''(\omega)]$ of U_g. In the left part and the right part of Fig. 7, we display in double logarithmic scales the $[G''(\omega)]$ of U_g of $f = 3$ and $f = 4$, respectively, for different values of the stiffness parameter q. Here we keep the generation fixed by taking $g = 6$ and vary the stiffness parameter by increasing q from the pure Rouse (fully-flexible) case, $q = 0$, to the semiflexible case $q = 0.888$. From Fig. 7, it is easy to observe that in both Rouse case and semiflexible case, for very low frequencies ω, we have $[G''(\omega)] \sim \omega^1$; and that for very high frequencies ω, we have $[G''(\omega)] \sim \omega^{-1}$. Note that these well-known universal scaling laws hold for nearly all finite polymer networks[3]. Hence, the particular structure of a polymer leaves its significant fingerprints in the intermediate region. Here, in the double-logarithmic scale, nearly no straight lines are observable in the intermediate region of $[G''(\omega)]$, which means that it appears a nonscaling behavior in this region. In Fig. 7, we can infer from the curve, that differences in the stiffness parameter q affect the intermediate behavior of $[G''(\omega)]$ dramatically.

As it is shown in Fig. 7, the $[G''(\omega)]$-curves show a major peak in the intermediate region. With increasing stiffness parameter q, the $[G''(\omega)]$ curve starts to bend downwards in the in-between region. The semiflexibility is reflected in the $[G''(\omega)]$ through a local minimum and a second minor peak appearing at intermediate frequencies. The reason for this fact lies in the unique spectra distribution of the polymer network. In Fig. 5, we can see that there is a clear gap in each spectrum near the value 1.0: In the left part of Fig. 5, for $q = 0.333$, the largest eigenvalue smaller than 1.0 is $\lambda \approx 0.9808$, and the smallest eigenvalue greater than 1.0 is $\lambda \approx 5.1127$, thus this gap is about 4.1319, while it is equal to 7.489 for $q = 0.666$ and to 20.947 for $q = 0.888$, respectively. Hence, the gap in the spectra depends strongly on q, growing with q dramatically. Moreover, with increasing stiffness parameter q, the $[G''(\omega)]$ curves get wider especially in the high frequency region, which is also observed before in a series of semiflexible polymer networks[23,33,34]. The explanation for this phenomenon lies in the broadening of the eigenvalue spectra with growing stiffness parameter q.

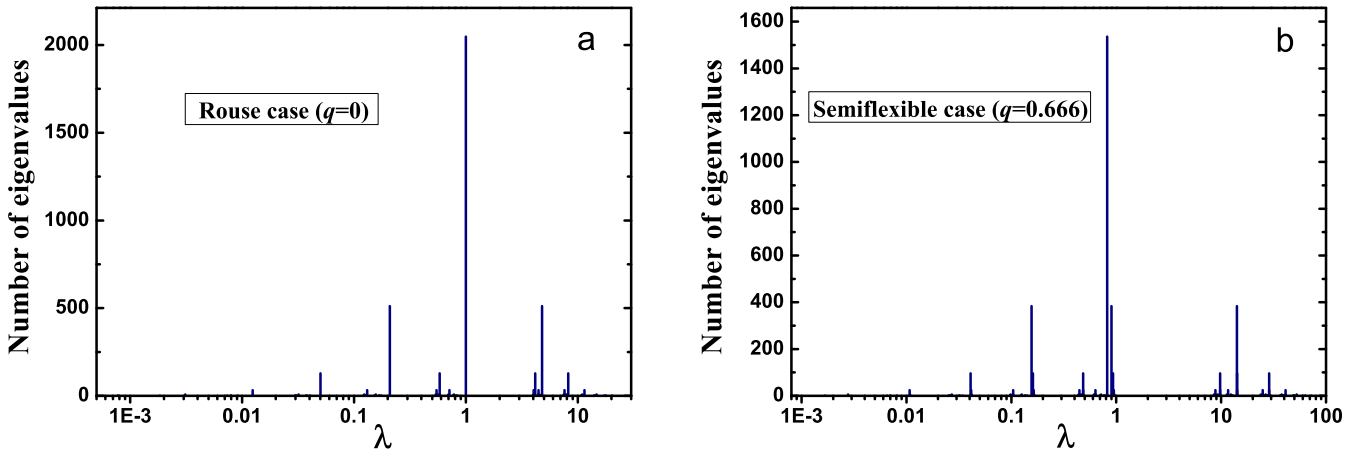

Figure 6 | Number of distinct eigenvalues for polymer network U_g of generation $g = 6$ and functionality $f = 3$ for different degrees of stiffness q, with $q = 0$ (a) and $q = 0.666$ (b).

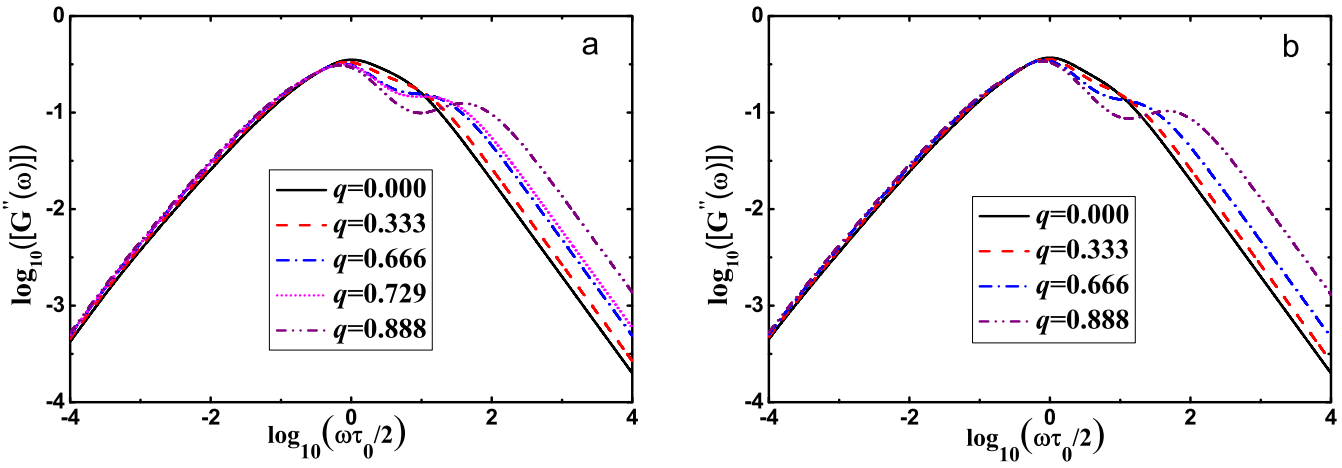

Figure 7 | **Reduced loss moduli $[G''(\omega)]$ for U_g of functionality $f = 3$ (a) and $f = 4$ (b), based on the spectra of Fig. 6.**

In order to have a deeper understanding of $[G''(\omega)]$ curves, in Fig. 8 we plot the derivative $\alpha(\omega) = \frac{d\log_{10}[G'(\omega)]}{d\log_{10}(\omega\tau_0/2)}$ for the $[G''(\omega)]$ curves of Fig. 7 as a function of $\log_{10}(\omega\tau_0/2)$ in a simple logarithmic scale. As we can see from Fig. 8, the value of $\alpha(\omega)$ starts to decrease from 1.0 in the low frequency domain and falls down around $\omega\tau_0/2 \approx 1$. In the intermediate region, the value again goes up rapidly and then it descends to the value -1.0 in the high frequency. From the left part of Fig. 8, we can see that there are 3 intersection points between the straight line $\alpha(\omega) = 0$ and the $\alpha(\omega)$ curve for the $q > 0.729$, which indicates that a local minimum of the $[G''(\omega)]$ can be observed when $q > 0.729$. Moreover, the intersection points between these two curves shift to higher ω-region with growing stiffness parameter, which means that, in the $[G''(\omega)]$, the local minimum and the second minor peak shift to the high frequency region with increasing q. This feature is also apparent from Fig. 7.

We conclude that the mechanical relaxation functions show that the networks U_g belong to the class of polymeric structures whose dynamics does not scale in the intermediate frequency (or time) domain. Such a non-scaling behavior show other well-known structures, namely dendrimers and some structurally disordered SFNs (SDSFNs)[12,15,27,33,41]. Nevertheless, their relaxation dynamics differs from that of the U_g, especially for the semiflexible case. Namely, the $[G''(\omega)]$ of semiflexible dendrimers show a considerable broadening towards both low and high frequencies[33], whereas for U_g the curves in the low-frequency domain display only little differences. Hence the relaxation at the large scales is for the U_g networks less affected by stiffness than for dendrimers. In comparison to SDSFNs[41], inclusion of stiffness leads for several SDSFNs to a local minimum in $[G''(\omega)]$ which, however, considerably less pronounced than by U_g. This is also obvious from the inspection of the corresponding local slopes, which for SDSFNs do not show big jumps as in Fig. 8[41].

Discussion

In summary, we presented a systematic theoretical investigation of the dynamic properties of a family of growing semiflexible treelike polymer networks in the framework of STP. The main goal of this article is to explore the impact of various polymer structures and of the different degrees of stiffness q, on the dynamic behavior of the polymer networks. To achieve this goal, we analyzed the dynamical matrix for the polymer networks and characterized their spectra. We succeeded to obtain a large part of the spectra analytically.

Based on the eigenvalue spectra, we have investigated the mechanical relaxation forms for the semiflexible polymer networks. In the in-between region, $[G''(\omega)]$ curve shows a nonscaling behavior, while in the very low and very high frequency, it shows ω^{-1} and ω^{1} behaviors respectively. Moreover, it turns out that the relaxation behavior is very sensitive to the stiffness. Indeed, with the increasing stiffness parameter q, the $[G''(\omega)]$ curves get broader especially in the high frequency domain (showing that the stiffness is very important at the local scales) and they start to show a local minimum and another minor peak in the in-between region. Such a distinct qualitative

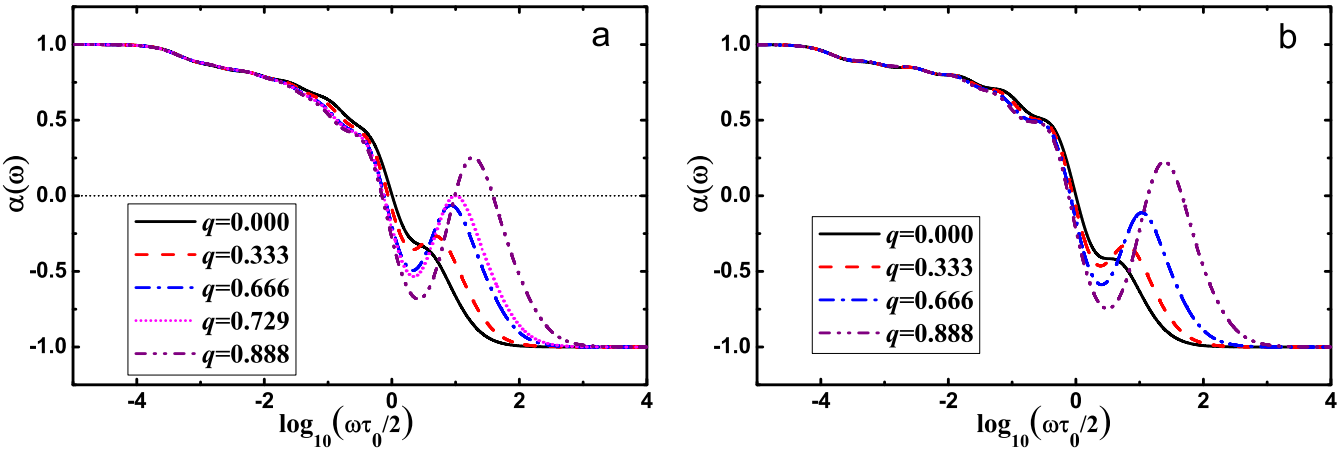

Figure 8 | **The corresponding slopes $\alpha(\omega)$ of reduced loss moduli $[G''(\omega)]$ for U_g of functionality $f = 3$ (a) and $f = 4$ (b), plotted for different degrees of stiffness.**

behavior is observed when the stiffness parameter q gets higher than 0.729 (for $f = 3$), as it follows from the analysis of the derivative for the $[G''(\omega)]$. These observations show that the considered networks U_g belong to the same class as the well-known, extensively synthesized[42] dendrimers. As we have found, however, the semiflexibility allows one to distinguish the U_g networks from dendrimers and from other representatives of the common class. We hope that recent progress in the synthesis, in particular, the realization of dendrimers with hypermonomers (monomers with high number of functional groups) and with monomers consisting of both active and inactive groups[42], will pave the way to the compounds with the properties of U_g. Finally, it is expected that the methods presented here can be extended to other classes of large semiflexible polymer networks.

Methods

Modelling Semiflexiblity. The polymer structure is modeled as a network, which consists of N beads located at $\boldsymbol{r}_i (i = 1 \cdots N)$ connected by springs (bonds)

$$\boldsymbol{l}_a = \boldsymbol{r}_i - \boldsymbol{r}_j. \tag{43}$$

We can express the transformation (43) from the bond to the positions' variables by the incidence matrix $\mathbf{G}$[38],

$$\boldsymbol{l}_a \equiv \sum_k \left(\mathbf{G}^{\mathrm{T}}\right)_{ak} \boldsymbol{r}_k. \tag{44}$$

Here the $\mathbf{G}^{\mathrm{T}}$ is the transposed matrix to $\mathbf{G}$; the matrix $\mathbf{G} = (G_{ia})$ has nonzero entries only $G_{ja} = -1$ and $G_{ia} = 1$, where the bond a starts in bead j and ends in bead i.

For the fully flexible polymers, the potential energy between beads is purely harmonic, so that it is diagonal in the bonds,

$$V_{fl}(\{\boldsymbol{l}_a\}) = \frac{K}{2}\sum_a \boldsymbol{l}_a^2. \tag{45}$$

Here the sum runs over all the bonds that build up the polymer. In equation (45), the spring constant K equals $3k_BT/l^2$, where k_B denotes the Boltzmann constant, T is the temperature, and l^2 is the mean-square bond length (all bonds are of the same mean-square length). From equation (45) it follows that in the GGS picture the equilibrium bond-bond correlations $\langle \boldsymbol{l}_a \cdot \boldsymbol{l}_b \rangle_{fl}$ evaluated with respect to the Boltzmann distribution $\exp(-V_{fl}/k_BT)$ vanish[24].

However, for semiflexible polymers, the bonds are correlated, i.e. their orientations are not arbitrary. In order to account for this feature, as discussed in Ref. 24, one may extend equation (45) and use the generalized potential energy V_s:

$$V_s(\{\boldsymbol{l}_a\}) = \frac{K}{2}\sum_{a,b} W_{ab}\, \boldsymbol{l}_a \cdot \boldsymbol{l}_b, \tag{46}$$

Under the assumption that $\boldsymbol{l}_a$ follow normal distribution, the average of $\langle \boldsymbol{l}_a \cdot \boldsymbol{l}_b \rangle$ with respect to the Boltzmann distribution is

$$\langle \boldsymbol{l}_a \cdot \boldsymbol{l}_b \rangle_s = l^2 \left(\boldsymbol{W}^{-1}\right)_{ab} \tag{47}$$

In this way one has the relation between the potential energy and the mean scalar products of bonds. For the latter the following traditional[23–32] conditions are taken: First, the mean-squared length is

$$\langle \boldsymbol{l}_a \cdot \boldsymbol{l}_a \rangle_s = l^2. \tag{48}$$

For adjacent bonds $\boldsymbol{l}_a$ and $\boldsymbol{l}_b$ which are connected by the bead i one has

$$\langle \boldsymbol{l}_a \cdot \boldsymbol{l}_b \rangle_s = \pm l^2 q_i. \tag{49}$$

Here the parameter q_i reflects the stiffness degree of the bead i; the plus or minus sign of q_i depends on the connection of bonds $\boldsymbol{l}_a$ and $\boldsymbol{l}_b$, e.g. the plus sign holds for a head to tail arrangement whereas the minus sign appears in the other cases. In a three-dimensional space q_i is restricted by $q_i < 1/(f_i - 1)$, where f_i is the functionality of the bead i[40]. Another limit $q_i = 0$ leads to a fully-flexible model. For non-adjacent bonds $\boldsymbol{l}_a$ and $\boldsymbol{l}_c$, one has as in the freely rotating chain model,

$$\langle \boldsymbol{l}_a \cdot \boldsymbol{l}_c \rangle = \langle \boldsymbol{l}_a \cdot \boldsymbol{l}_{b_1} \rangle \langle \boldsymbol{l}_{b_1} \cdot \boldsymbol{l}_{b_2} \rangle \ldots \langle \boldsymbol{l}_{b_k} \cdot \boldsymbol{l}_c \rangle l^{-2k}. \tag{50}$$

Here $(a, b_1, b_2, \ldots, b_k, c)$ denotes the unique, shortest path from bond $\boldsymbol{l}_a$ to bond $\boldsymbol{l}_c$.

Under the conditions of equations (48) – (50), the potential energy $V_s(\{\boldsymbol{l}_a\})$ of equation (4) has an analytic-closed form[24]. In order to get the V_s the frame of beads, we substitute equation (44) into equation (49), leading to

$$V_s(\{\boldsymbol{r}_i\}) = \frac{K}{2}\sum_{k,n} A_{kn}^{\mathrm{STP}}\, \boldsymbol{r}_k \cdot \boldsymbol{r}_n, \tag{51}$$

where $\mathbf{A}^{\mathrm{STP}}$ is the so-called dynamical matrix and is given by $\mathbf{A}^{\mathrm{STP}} = \mathbf{G}\mathbf{W}\mathbf{G}^{\mathrm{T}}$. Based on equation (51), one can readily write down the equation of motions (2), where the structure of $\mathbf{A}^{\mathrm{STP}}$ is presented in equations (3)∼ (5).

Spectra of flexible polymer networks U_g. According to the construction of U_g, the dynamical matrix $\mathbf{A}^{\mathrm{GGS}}$ of fully-flexible U_g is the connectivity matrix and is given by[35]

$$\mathbf{A}_g^{\mathrm{GGS}} = \begin{pmatrix} \mathbf{A}_{g-1}^{\mathrm{GGS}} + f\mathbf{I}_{g-1} & -\mathbf{I}_{g-1} & -\mathbf{I}_{g-1} & \cdots & -\mathbf{I}_{g-1} \\ -\mathbf{I}_{g-1} & \mathbf{I}_{g-1} & 0 & \cdots & 0 \\ -\mathbf{I}_{g-1} & 0 & \mathbf{I}_{g-1} & \cdots & 0 \\ \vdots & \vdots & \vdots & \vdots & \vdots \\ -\mathbf{I}_{g-1} & 0 & 0 & \cdots & \mathbf{I}_{g-1} \end{pmatrix}, \tag{52}$$

whose characteristic polynomial satisfies following recursive relation[35]

$$Q_g(\lambda) = (\lambda - 1)^{f(f+1)^{g-1}} Q_{g-1}\left(\lambda - f - \frac{f}{\lambda - 1}\right). \tag{53}$$

We use notation FE_g to represent the eigenvalues set of matrix $\mathbf{A}_g^{\mathrm{GGS}}$. Note that the polymer networks have $(f+1)^g$ nodes, which indicted that there are $(f+1)^g$ eigenvalues in the set FE_g. Based on the recursive relation of the characteristic polynomial $Q(\lambda)$, FE_g can be divided into two subset $FE1_g$ and $FE2_g$. That is to say, $FE_g = FE1_g \cup FE2_g$, where $FE1_g$ contains eigenvalue 1 with multiplicity $(f-1)(f+1)^{g-1}$. Thus,

$$FE1_g = \underbrace{\{1,1,1,\cdots,1,1\}}_{(f-1)(f+1)^{g-1}}. \tag{54}$$

$FE2_g$ consists the remaining $2(f+1)^{g-1}$ eigenvalues which are determined by the following equation[35]

$$\lambda - f - \frac{f}{\lambda - 1} = \lambda_i^{g-1}, \tag{55}$$

where λ_i^{g-1} is an arbitrary eigenvalue in the set FE_{g-1}. Note that equation (55) have two roots for each λ_i^{g-1}. Thus, each eigenvalue in FE_{g-1} generates two new eigenvalues in $FE2_g$. And the FE_g set can be fully determined by recursively applying above two equations.

Similarly to the eigenvalues, the eigenvectors of $\mathbf{A}_g^{\mathrm{GGS}}$ can be determined from those of $\mathbf{A}_{g-1}^{\mathrm{GGS}}$. Let $\boldsymbol{v}$ denote the eigenvector, whose corresponding eigenvalue is λ. $\boldsymbol{v}$ can be expressed as

$$\boldsymbol{v} = \begin{pmatrix} \boldsymbol{v}_1 \\ \boldsymbol{v}_2 \\ \boldsymbol{v}_3 \\ \vdots \\ \boldsymbol{v}_{f+1} \end{pmatrix}, \tag{56}$$

where all $\boldsymbol{v}_i$ of the vector $\boldsymbol{v}$ have same sizes. We can solve equation $\left(\lambda\mathbf{I} - \mathbf{A}_g^{\mathrm{GGS}}\right)\boldsymbol{v} = 0$ to determine the vector $\boldsymbol{v}$. We distinguish two cases: $\lambda \in FE1_g$ and $\lambda \in FE2_g$, which will be addressed as follows.

For the first case of $\lambda \in FE1_g$, where all $\lambda = 0$, the equation $\left(\lambda\mathbf{I} - \mathbf{A}_g^{\mathrm{GGS}}\right)\boldsymbol{v} = 0$ leads to the following equations:

$$\boldsymbol{v}_1 = 0 \tag{57}$$

$$\boldsymbol{v}_2 + \boldsymbol{v}_3 + \cdots + \boldsymbol{v}_{f+1} = 0. \tag{58}$$

For the second case of $\lambda \in FE2_g$, we can have following relations.

$$\left[(\lambda - f)\mathbf{I}_{g-1} - \mathbf{A}_{g-1}^{\mathrm{GGS}}\right]\boldsymbol{v}_1 + \boldsymbol{v}_2 + \cdots + \boldsymbol{v}_{f+1} = 0, \tag{59}$$

$$\boldsymbol{v}_1 + (\lambda - 1)\boldsymbol{v}_i = 0 \quad (2 \le i \le f+1). \tag{60}$$

Resolving equations (59) and (60) to find

$$\left[\left(\lambda - f - \frac{f}{\lambda - 1}\right)\mathbf{I}_{g-1} - \mathbf{A}_{g-1}^{\mathrm{GGS}}\right]\boldsymbol{v}_1 = 0, \tag{61}$$

$$\boldsymbol{v}_i = -\frac{1}{\lambda - 1}\boldsymbol{v}_1 \quad (2 \le i \le f+1), \tag{62}$$

which shows that all the $\boldsymbol{v}_i (2 \le i \le f+1)$ have same values and are uniquely determined by the $\boldsymbol{v}_1$. Equation (61) together with equation (55) indicates that $\boldsymbol{v}_i$ is an eigenvector of matrix $\mathbf{A}_g^{\mathrm{GGS}}$ associated with the eigenvalue $\lambda - f - \frac{f}{\lambda - 1}$ determined

by λ_i^{g-1}. Thus, eigenvector $\boldsymbol{v}$ can be expressed as

$$\boldsymbol{v}=\begin{pmatrix}\boldsymbol{v}_1\\ \boldsymbol{v}_2\\ \boldsymbol{v}_3\\ \vdots\\ \boldsymbol{v}_{f+1}\end{pmatrix}=\begin{pmatrix}\boldsymbol{v}_1\\ -\frac{1}{\lambda-1}\boldsymbol{v}_1\\ -\frac{1}{\lambda-1}\boldsymbol{v}_1\\ \vdots\\ -\frac{1}{\lambda-1}\boldsymbol{v}_1\end{pmatrix}, \tag{63}$$

which implies that $\boldsymbol{v}$ satisfies the following relation:

$$\boldsymbol{v}_2=\boldsymbol{v}_3=\boldsymbol{v}_4=\cdots=\boldsymbol{v}_{f+1}. \tag{64}$$

1. Matyjaszewski, K. & Tsarevsky, N. V. Nanostructured functional materials prepared by atom transfer radical polymerization. *Nat. Chem.* **1**, 276–288 (2009).
2. Urban, M. W. Stratification, stimuli-responsiveness, self-healing, and signaling in polymer networks. *Prog. Polym. Sci.* **34**, 679–687 (2009).
3. Gurtovenko, A. A. & Blumen, A. Generalized gaussian structures: Models for polymer systems with complex topologies. *Adv. Polym. Sci.* **182**, 171–282 (2005).
4. Rouse, P. E. A theory of the linear viscoelastic properties of dilute solutions of coiling polymers. *J. Chem. Phys.* **21**, 1272–1280 (1953).
5. Cai, C. & Chen, Z. Y. Rouse dynamics of a dendrimer model in the ϑ condition. *Macromolecules* **30**, 5104–5117 (1997).
6. Gurtovenko, A. A. & Gotlib, Y. Y. Intra- and interchain relaxation processes in meshlike polymer networks. *Macromolecules* **31**, 5756–5770 (1998).
7. Gurtovenko, A. A. & Gotlib, Y. Y. Viscoelastic dynamic properties of meshlike polymer networks: Contributions of intra-and interchain relaxation processes. *Macromolecules* **33**, 6578–6587 (2000).
8. Blumen, A. & Jurjiu, A. Multifractal spectra and the relaxation of model polymer networks. *J. Chem. Phys.* **116**, 2636–2641 (2002).
9. Koslowski, T., Jurjiu, A. & Blumen, A. Models of irregular hyperbranched polymers: Topological disorder and mechanical response. *Macromol. Theory Simul.* **15**, 538–545 (2006).
10. Galiceanu, M. & Blumen, A. Spectra of Husimi cacti: Exact results and applications. *J. Chem. Phys.* **127**, 134904 (2007).
11. Gurtovenko, A. A., Gotlib, Y. Y. & Blumen, A. Rouse dynamics of polymer networks bearing dendritic wedges. *Macromolecules* **35**, 7481–7491 (2002).
12. Gurtovenko, A. A., Markelov, D. A., Gotlib, Y. Y. & Blumen, A. Dynamics of dendrimerbased polymer networks. *J. Chem. Phys.* **119**, 7579–7590 (2003).
13. Blumen, A., Jurjiu, A., Koslowski, T. & von Ferber, C. Dynamics of Vicsek fractals, models for hyperbranched polymers. *Phys. Rev. E* **67**, 061103 (2003).
14. Blumen, A., Von Ferber, C., Jurjiu, A. & Koslowski, T. Generalized Vicsek fractals: Regular hyperbranched polymers. *Macromolecules* **37**, 638–650 (2004).
15. Galiceanu, M. Relaxation dynamics of scale-free polymer networks. *Phys. Rev. E* **86**, 041803 (2012).
16. Galiceanu, M. Hydrodynamic effects on scale-free polymer networks in external fields. *J. Chem. Phys.* **140**, 034901 (2014).
17. Jespersen, S., Sokolov, I. M. & Blumen, A. Small-world Rouse networks as models of crosslinked polymers. *J. Chem. Phys.* **113**, 7652–7655 (2000).
18. Gurtovenko, A. A. & Blumen, A. Relaxation of disordered polymer networks: Regular lattice made up of small-world Rouse networks. *J. Chem. Phys.* **115**, 4924–4929 (2001).
19. Sokolov, I. M., Klafter, J. & Blumen, A. Fractional Kinetics. *Physics Today* **55**, 11, 48–54 (2002).
20. Siggia, E. D., Bustamante, C., Marko, J. F. & Smith, S. B. Entropic elasticity of λ-phage DNA. *Science* **265**, 1599–1600 (1994).
21. Käs, J. *et al.* F-actin, a model polymer for semiflexible chains in dilute, semidilute, and liquid crystalline solutions. *Biophys. J.* **70**, 609–625 (1996).
22. Götter, R., Kroy, K., Frey, E., Bärmann, M. & Sackmann, E. Dynamic light scattering from semidilute actin solutions: a study of hydrodynamic screening, filament bending stiffness, and the effect of tropomyosin/troponin-binding. *Macromolecules* **29**, 30–36 (1996).
23. Dolgushev, M., Berezovska, G. & Blumen, A. Branched semiflexible polymers: theoretical and simulation aspects. *Macromol. Theory Simul.* **20**, 621–644 (2011).
24. Dolgushev, M. & Blumen, A. Dynamics of semiflexible treelike polymeric networks. *J. Chem. Phys.* **131**, 044905 (2009).
25. Dolgushev, M., Guérin, T., Blumen, A., Bénichou, O. & Voituriez, R. Gaussian semiflexible rings under angular and dihedral restrictions. *J. Chem. Phys.* **141**, 014901 (2014).
26. Kumar, A. & Biswas, P. Dynamics of semiflexible dendrimers in dilute solutions. *Macromolecules* **43**, 7378–7385 (2010).
27. Kumar, A. & Biswas, P. Intramolecular relaxation dynamics in semiflexible dendrimers. *J. Chem. Phys.* **134**, 214901 (2011).
28. Kumar, A. & Biswas, P. Conformational transitions in semiflexible dendrimers induced by bond orientations. *J. Chem. Phys.* **137**, 124903 (2012).
29. Markelov, D. A., Dolgushev, M., Gotlib, Y. Y. & Blumen, A. NMR relaxation of the orientation of single segments in semiflexible dendrimers. *J. Chem. Phys.* **140**, 244904 (2014).
30. Bixon, M. & Zwanzig, R. Optimized Rouse–Zimm theory for stiff polymers. *J. Chem. Phys.* **68**, 1896–1902 (1978).
31. Winkler, R. G., Reineker, P. & Harnau, L. Models and equilibrium properties of stiff molecular chains. *J. Chem. Phys.* **101**, 8119–8129 (1994).
32. Guenza, M. & Perico, A. A reduced description of the local dynamics of star polymers. *Macromolecules* **25**, 5942–5949 (1992).
33. Fürstenberg, F., Dolgushev, M. & Blumen, A. Analytical model for the dynamics of semiflexible dendritic polymers. *J. Chem. Phys.* **136**, 154904 (2012).
34. Fürstenberg, F., Dolgushev, M. & Blumen, A. Dynamics of semiflexible regular hyperbranched polymers. *J. Chem. Phys.* **138**, 034904 (2013).
35. Liu, H. X. & Zhang, Z. Z. Laplacian spectra of recursive treelike small-world polymer networks: Analytical solutions and applications. *J. Chem. Phys.* **138**, 114904 (2013).
36. Ferry, J. D. *Viscoelastic properties of polymers* (John Wiley & Sons, 1980).
37. Doi, M. & Edwards, S. F. *The theory of polymer dynamics* (Clarendon, Oxford, 1986).
38. Biggs, N. *Algebraic graph theory* (Cambridge university press, 1993).
39. Watts, D. J. & Strogatz, S. H. Collective dynamics of 'small-world' networks. *Nature* **393**, 440–442 (1998).
40. Mansfield, M. L. & Stockmayer, W. H. Unperturbed dimensions of wormlike stars. *Macromolecules* **13**, 1713–1715 (1980).
41. Galiceanu, M., Reis, A. S. & Dolgushev, M. Dynamics of semiflexible scale-free polymer networks. *J. Chem. Phys.* **141**, 144902 (2014).
42. Sowinska, M. & Urbanczyk-Lipkowska, Z. Advances in the chemistry of dendrimers. *New J. Chem.* **38**, 2168–2203 (2014).

Acknowledgments

Authors thank Prof. A. Blumen for helpful discussions. This work was supported by the National Natural Science Foundation of China under Grant No. 11275049. M.D. acknowledges DFG through Grant No. Bl 142/11-1 and through IRTG "Soft Matter Science" (GRK 1642/1).

Author contributions

Y.Q., M.D. and Z.Z.Z. designed the research, performed the research, and wrote the manuscript.

Additional information

Competing financial interests: The authors declare no competing financial interests.

How to cite this article: Qi, Y., Dolgushev, M. & Zhang, Z. Dynamics of semiflexible recursive small-world polymer networks. *Sci. Rep.* **4**, 7576; DOI:10.1038/srep07576 (2014).